24th International Conference on Renewable Energies and Power Quality (ICREPQ'26)
Santander (Spain), 10th to 12th June 2026
ISBN-13: 978-84-09-82044-3

The application of orthogonal vector theory to optimize the coordination between a 3-level inverter and a 2-level inverter

A. Muc[1]

[1] Department of Ship Automation
Gdynia Maritime University
Morska St. 83, 81-225 Gdynia (Poland)
Phone/Fax number:+48 505 279 861, e-mail: **a.muc@we.umg.edu.pl**

Abstract. This article demonstrates the potential application of orthogonal vector theory to the design and control of complex systems with three-phase inverters. The paper presents the interaction of a three-level inverter with a two-level inverter using two control strategies. The obtained results are presented in the form of simulation studies. The analyses show that the complex voltage inverter with a simplified control strategy allows for higher RMS voltage values with lower THD.

Key words. space vector; vector orthogonality; three-phase OVT inverter; fundamental harmonic.

1. Introduction

The development of renewable energy sources and electromobility is currently a key factor influencing progress in power electronics, leading to the emergence of circuit solutions intended for cooperation between various converters and for electrical energy conditioning. These aspects are essential when analysing the possibilities of integrating RES (Renewable Energy Source) systems with existing power grids [1].

The conversion of DC into AC is one of the primary objectives of modern power electronics. This requirement is present in AC drive systems as well as in renewable energy applications such as smart grids. In both areas, the fundamental parameters to be controlled are voltage amplitude and frequency, although their regulation ranges differ significantly. A typical AC drive control system employs an inverter as a DC/AC converter. The widely used PWM (pulse-width modulation) technique results in an output voltage composed of rectangular pulses. Consequently, obtaining a sinusoidal voltage waveform usually requires the application of a low-pass filter capable of extracting the fundamental harmonic component [3].

In such systems, the inverter constitutes one of the most crucial elements. Reference [4] provides a comprehensive overview of inverter types used in different applications and power system configurations. In general, conventional voltage-source inverters are applied, generating two voltage levels [5]. In contrast, applications requiring higher power levels (e.g., on-shore power supply systems) often utilize multilevel inverters (MLIs). An MLI is a converter topology in which multiple power electronic devices are interconnected and supplied from DC sources to produce an output waveform with several voltage levels [6,7]. These converters are attractive due to advantages such as reduced switching voltage stress, lower dv/dt ratios, improved reliability, lower costs, reduced complexity, better THD performance, and high efficiency in practical applications [8,9].

Since the introduction of multilevel inverters, numerous structural modifications and control strategies have been proposed. However, these developments have led to increased circuit complexity, higher weight and cost, greater stress on switching devices, as well as electromagnetic compatibility (EMC) and electromagnetic interference (EMI) issues, and additional losses. As a result, system performance may deteriorate, influencing power quality in distribution networks. Therefore, conventional two-level inverters remain widely used, particularly in low-power applications [4].

Various modulation techniques are employed to develop inverter control strategies [10,11]. A large portion of these methods is based on modifications of PWM schemes. However, PWM-based approaches typically increase switching losses in power electronic devices [12–14].

As previously noted, the application of multilevel inverters together with suitable control strategies enables the generation of multi-level output voltages. Such voltages are generally associated with lower total harmonic distortion (THD) and improved power quality [15]. Nevertheless, achieving these benefits requires complex inverter topologies and sophisticated control methods involving a large number of switching elements [16].

The design of converter systems consisting of multiple inverters in a three-phase configuration necessitates analysis of solutions that enable their integration within a single system. For this purpose, systems based on transformers, multi-winding transformers, and magnetically coupled reactors have been investigated and compared [17–18].

At the same time, there exist promising concepts related to DC/AC converters composed of two inverters, referred to in this work as orthogonal-vectors-controlled inverters (OVTs). The advantages and limitations of control methods based on orthogonal vectors have been discussed in [19,20]. The initial control approach for the auxiliary inverter exhibited limited efficiency, mainly due to the use of a transformer transferring relatively long pulses. To address this drawback, a modified control concept for the auxiliary inverter was proposed in [21]. The approach presented in [21] introduces an improved OVT control method, resulting in a significant reduction of the transformer size used as a summing element.

This paper presents a novel approach to the cooperation between a three-level inverter and a two-level inverter. In contrast to earlier solutions based solely on two-level inverters, the proposed system enables higher power transfer, reduced THD, and offers additional control capabilities.

2. The concept of orthogonal vectors in the control of a set of voltage inverters

The theory of orthogonal vectors was developed on the assumption that both inverters, i.e. the main inverter (MI) and the auxiliary inverter (AI), are three-phase two-level inverters. Therefore, each of these inverters generates the same number of spatial vectors, but these are phase-shifted by an angle of π/2 relative to one another.

The basic block diagram of the OVT inverter is presented in Figure 1. The operating principle and performance characteristics of this inverter have been described in [14,21]. In this configuration, the main inverter is capable of generating 32 space voltage vectors of comparable magnitude.

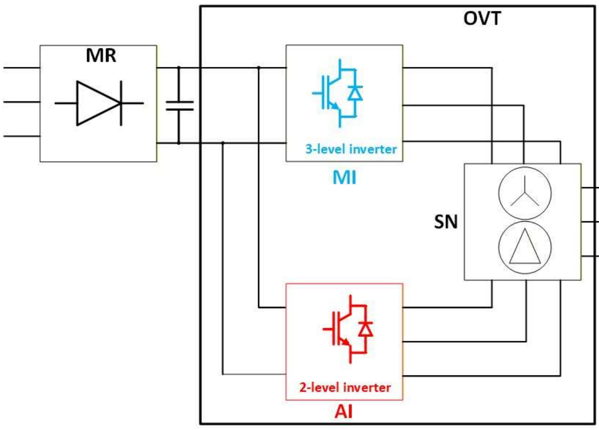

Fig. 1. Schematic diagram of the OVT inverter, where: SN – summing node, MR – main rectifier.

The individual inverters are connected through a system of single-phase transformers and supplied from a common DC voltage source. A key element of the topology is the summing node implemented using three single-phase transformers. The main inverter and the load are connected in a star configuration, whereas the auxiliary inverter is connected in a delta arrangement. As a consequence, the phase voltage of the main inverter is influenced by the line-to-line voltage generated by the auxiliary inverter.

Next figure 2 determines the rule of vector creation. The vectors are denoted as:

- V_{MIm} — the main inverter voltage vector with *m* number of vectors,
- V_{AIn} —the auxiliary inverter voltage vector with *n* number of vectors,,
- V_{OVTk} — the OVT inverter voltage vector with k number of vectors.

In the case of the original configuration, consisting of two identical three-phase and two-level voltage inverters, each of them allowed to generate 6 non-zero space vectors, which meant that m = n.

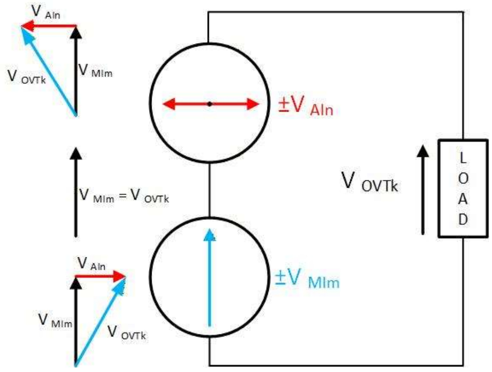

Fig.2. The formation concept of vectors V_{OVTk}.

In every of six k-sectors of the stationary coordinate system plane (α, β) the OVT inverter generates a sequence of three voltage vectors: V_(OVT-), V_OVT, V_(OVT+), assigned to the k-th sector of the plane (α, β). The order of generation is described in equation (1):

$$\begin{aligned} \underset{\rightarrow OVTk-}{V} &= \underset{\rightarrow AIk}{V} + \underset{\rightarrow MIk}{V} \\ \underset{\rightarrow OVTk}{V} &= \underset{\rightarrow MIk}{V} \\ \underset{\rightarrow OVT}{V} &= \underset{\rightarrow AIk}{V} + \underset{\rightarrow MIk}{V} \end{aligned} \tag{1}$$

The symbol k⊕3 denotes the modulo 6 sum of the index k and the number 3. Assuming that m=n=6, the number k = 18. Expression (1) illustrates a control method based on the principle of orthogonal vector summation. In the stationary coordinate system (α, β) the active vectors of the component inverters are described by expressions (2).

$$\begin{cases} \underset{\rightarrow MIk}{V} = \left|\underset{\rightarrow MIk}{V}\right| e^{j\,\left[(k-1)\frac{\pi}{3} \pm 2\pi n\right]} \\ \underset{\rightarrow AIk}{V} = \pm\, jm \underset{\rightarrow MIk}{V} = \pm\, m \underset{\rightarrow MIk}{V} e^{j\frac{\pi}{2}} \end{cases} \tag{2}$$

According to equations (1, 2), the output space vectors of the OVT orthogonal converter are given by relations (3).

$$\begin{cases} \underset{\rightarrow OVk-}{V} = (1-jm)\underset{\rightarrow MIk}{V} = \sqrt{1+m^2}\underset{\rightarrow MIk}{V} e^{-j\cdot arctan\, m} \\ \underset{\rightarrow OVk}{V} = \underset{\rightarrow MIk}{V} = \left|\underset{\rightarrow MIk}{V}\right| e^{j\,\left[(k-1)\frac{\pi}{3} \pm 2k\,\pi\right]} \\ \underset{\rightarrow OVk+}{V} = (1+jm)\underset{\rightarrow MIk}{V} = \sqrt{1+m^2}\underset{\rightarrow MIk}{V} e^{j\cdot arctan\, m} \end{cases} \tag{3}$$

Figure 3 shows the space vectors for the MI and AI inverters when both inverters are three-phase, two-level voltage-source inverters. In this case, all active space vectors are equal one to another.

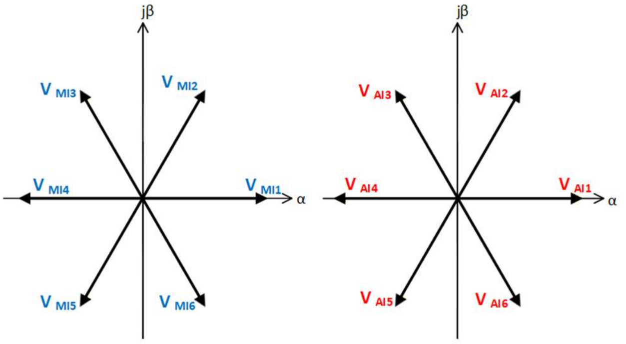

Fig.3. The spacer vectors V_{MIm} and V_{Ain}, when both inventers are three-phase, two-level voltage-source inverters.

Figure 4, on the other hand, shows the space vectors of the MI and AI inverters in a scenario where the MI inverter is a three-phase, three-level voltage-source inverter and the AI inverter is a three-phase, two-level voltage-source inverter. In this case, there has been a significant change in the space vectors for the MI inverter. In a three-level inverter, a greater number of space vectors of varying lengths can be generated. In the new inverter configuration, the number of space vectors for the MI and AI inverters is no longer equal and satisfies the inequality $m > n$. The remainder of this paper will consider precisely this new configuration of three-phase voltage-source inverters with different numbers of levels.

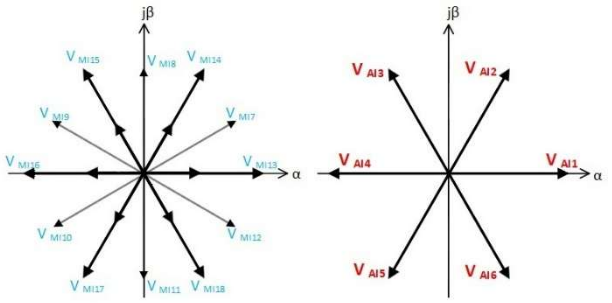

Fig.4. The spacer vectors V_{MIm} and V_{Ain} when one inverter is a three-level and the other is a two-level voltage inverter.

Figures 5 and 6 show the space vectors of both inverters and sample orthogonal vectors. Figures 5 and 6 also illustrate the vector switching sequence, from which it can be concluded that not all space vectors can be included in the control process, e.g., vectors marked MI7, MI8, MI9, MI10, MI11, MI12, etc., because they are not orthogonal to the auxiliary vector. Only the longest vectors (MI13, MI14, MI15, MI16, MI17, MI18) are considered in the control, which are also orthogonal to the auxiliary vectors, i.e., AI1, AI2, AI3, AI4, AI5, and AI6. Figures 5 and 6 also show that, for the MI inverter, shorter vectors can be distinguished from the longest vectors, which are ignored in the control. Further analysis may reveal that these can also be utilised, but at the current stage of work, the control focuses on the longest vectors, which ensure the highest efficiency of the OVT inverter.

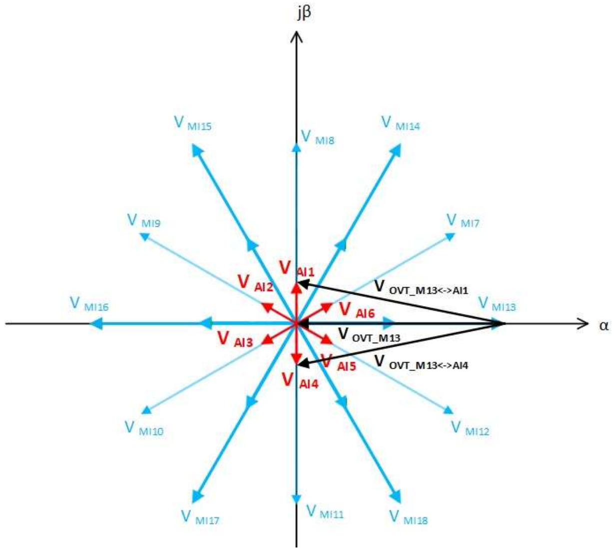

Fig.5. The formation concept of vectors V_{OVTk} – step 1.

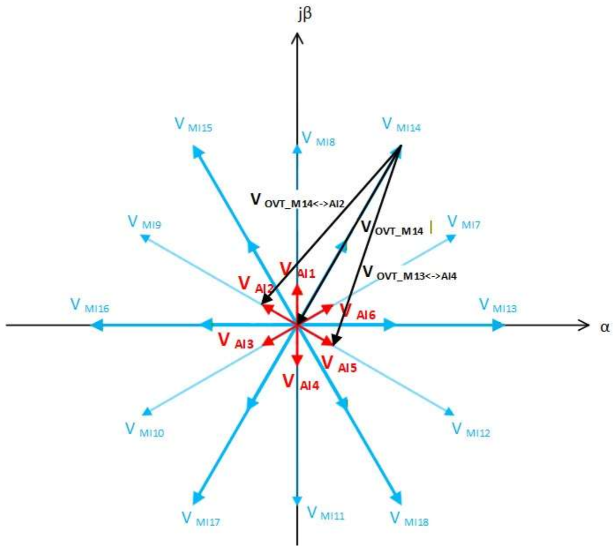

Fig.6. The formation concept of vectors V_{OVTk}– step 2.

Paper [22] describes a control strategy for a system comprising two three-phase inverters, where MI is a three-level inverter and AI is a two-level inverter, using standard space vectors for three-level and two-level inverters. A vector map showing the states of the transistor switches in the MI and AI inverters for phases a and b is shown in Figure 7. This control strategy requires as many as 36 state vectors for each inverter to obtain the voltage waveforms shown in Figure 11.

	0	1	2	3	4	5	6	7	8	9	10	11	12	13	14	15	16	17
TMIa1	0	0	0	1	1	1	1	1	1	1	1	1	1	1	1	1	1	1
TMIa2	1	1	1	1	1	1	1	1	1	1	1	1	1	1	1	1	1	1
TMIa3	1	1	1	0	0	0	0	0	0	0	0	0	0	0	0	0	0	0
TMIa4	0	0	0	0	0	0	0	0	0	0	0	0	0	0	0	0	0	0
TMIb1	0	0	0	0	0	0	0	0	0	0	0	0	0	0	0	1	1	1
TMIb2	0	0	0	0	0	0	0	0	0	0	0	0	1	1	1	1	1	1
TMIb3	1	1	1	1	1	1	1	1	1	1	1	1	1	1	1	0	0	0
TMIb4	1	1	1	1	1	1	1	1	1	1	1	1	0	0	0	0	0	0

	18	19	20	21	22	23	24	25	26	27	28	29	30	31	32	33	34	35
TMIa1	0	0	0	0	0	0	0	0	0	0	0	0	0	0	0	0	0	0
TMIa2	1	1	1	0	0	0	0	0	0	0	0	0	0	0	0	0	0	0
TMIa3	1	1	1	1	1	1	1	1	1	1	1	1	1	1	1	1	1	1
TMIa4	0	0	0	1	1	1	1	1	1	1	1	1	1	1	1	1	1	1
TMIb1	1	1	1	1	1	1	1	1	1	1	1	1	0	0	0	0	0	0
TMIb2	1	1	1	1	1	1	1	1	1	1	1	1	1	1	1	0	0	0
TMIb3	0	0	0	0	0	0	0	0	0	0	0	0	1	1	1	1	1	1
TMIb4	0	0	0	0	0	0	0	0	0	0	0	0	0	0	0	1	1	1

	0	1	2	3	4	5	6	7	8	9	10	11	12	13	14	15	16	17
TAIa1	1	1	1	0	1	1	0	0	0	0	0	1	1	1	1	1	1	0
TAIa2	0	0	0	1	0	0	1	1	1	1	1	0	0	0	0	0	0	1
TAIb1	1	1	1	1	1	0	0	0	0	0	0	1	1	1	1	0	1	1
TAIb2	0	0	0	0	0	1	1	1	1	1	1	0	0	0	0	1	0	0
TAIc1	1	1	1	1	1	0	0	0	0	1	0	0	1	1	1	1	1	0
TAIc2	0	0	0	0	0	1	1	1	1	0	1	1	0	0	0	0	0	1

	18	19	20	21	22	23	24	25	26	27	28	29	30	31	32	33	34	35
TAIa1	0	0	0	1	0	0	1	1	1	1	1	0	0	0	0	0	0	1
TAIa2	1	1	1	0	1	1	0	0	0	0	0	1	1	1	1	1	1	0
TAIb1	0	0	0	0	0	1	1	1	1	1	1	0	0	0	0	1	0	0
TAIb2	1	1	1	1	1	0	0	0	0	0	0	1	1	1	1	0	1	1
TAIc1	0	0	0	0	0	1	1	1	1	0	1	1	0	0	0	0	0	1
TAIc2	1	1	1	1	1	0	0	0	0	1	0	0	1	1	1	1	1	0

Fig.7. The vector map used for the control strategy of the inverters system described in [22].

A simplified version of the control strategy was also considered, in which the three-level inverter is controlled in a manner similar to that of a two-level inverter.

This control strategy (Fig. 8) significantly reduced the number of vectors required, while simultaneously enabling the inverter to produce phase and interphase output voltages characterized by low THD. In this case, only 18 state vectors are considered in the control strategy.

	0	1	2	3	4	5	6	7	8	9	10	11	12	13	14	15	16	17
TMIa1	1	1	1	1	1	1	1	1	1	0	0	0	0	0	0	0	0	0
TMIa2	1	1	1	1	1	1	1	1	1	0	0	0	0	0	0	0	0	0
TMIa3	0	0	0	0	0	0	0	0	0	1	1	1	1	1	1	1	1	1
TMIa4	0	0	0	0	0	0	0	0	0	1	1	1	1	1	1	1	1	1
TMIb1	0	0	0	0	0	0	1	1	1	1	1	1	1	1	1	0	0	0
TMIb2	0	0	0	0	0	0	1	1	1	1	1	1	1	1	1	0	0	0
TMIb3	1	1	1	1	1	1	0	0	0	0	0	0	0	0	0	1	1	1
TMIb4	1	1	1	1	1	1	0	0	0	0	0	0	0	0	0	1	1	1

	0	1	2	3	4	5	6	7	8	9	10	11	12	13	14	15	16	17
TAIa1	0	1	1	1	1	1	1	1	0	1	0	0	0	0	0	0	0	1
TAIa2	1	0	0	0	0	0	0	0	1	0	1	1	1	1	1	1	1	0
TAIb1	0	0	0	0	0	1	0	1	1	1	1	1	1	1	0	1	0	0
TAIb2	1	1	1	1	1	0	1	0	0	0	0	0	0	0	1	0	1	1

Fig.8. A vector map used for a simplified control strategy for the inverter system.

3. Inverter system model and simulation studies

To compare the control strategy described in [22] with its simplified version, a simulation model was constructed in PLECS, as shown in Figure 9. In the simulation model, a DC supply voltage of 400 V and a load of Ro= 10 Ω and Lo = 10 mH were assumed. For testing purposes, a voltage frequency of 50 Hz was assumed.

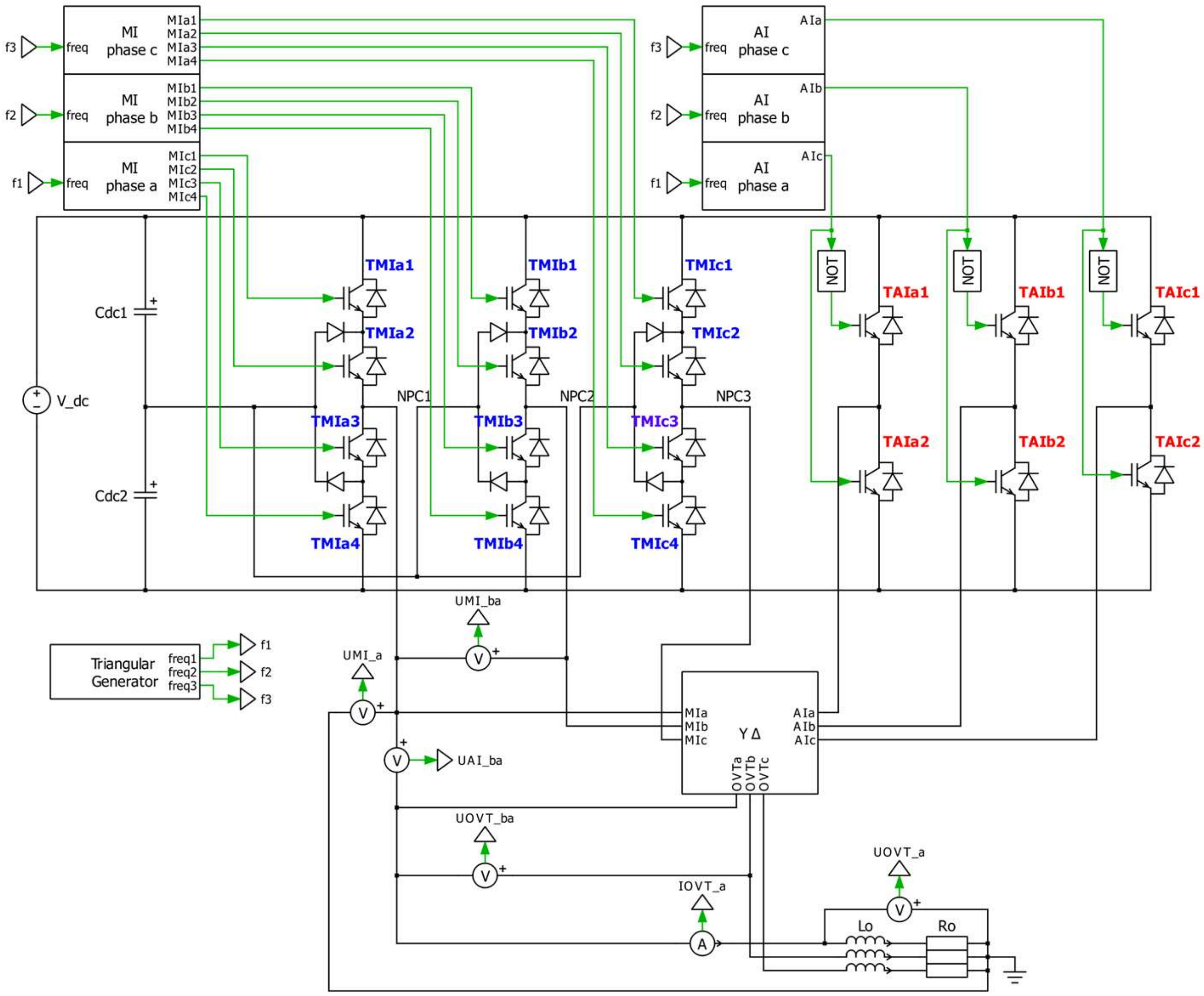

Fig. 9. A set of three-phase inverters, of which MI is a three-level inverter and AI is a two-level inverter.

An important element of the configuration is the summing node, which consists of single-phase transformers shown in Figure 10. A star connection is used on the MI inverter and load sides, and a delta connection on the AI inverter side. This node design ensures orthogonal voltages between the MI and AI inverters.

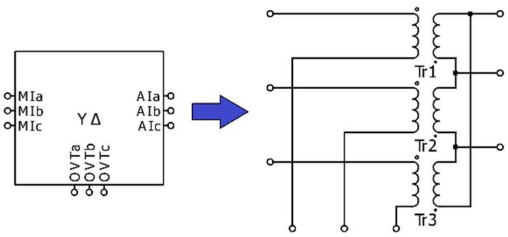

Fig.10. A summing node enabling the coordination of inverters of different levels.

Figure 11 shows the waveforms of selected voltages obtained for the control strategy described by the vector map shown in Figure 7.

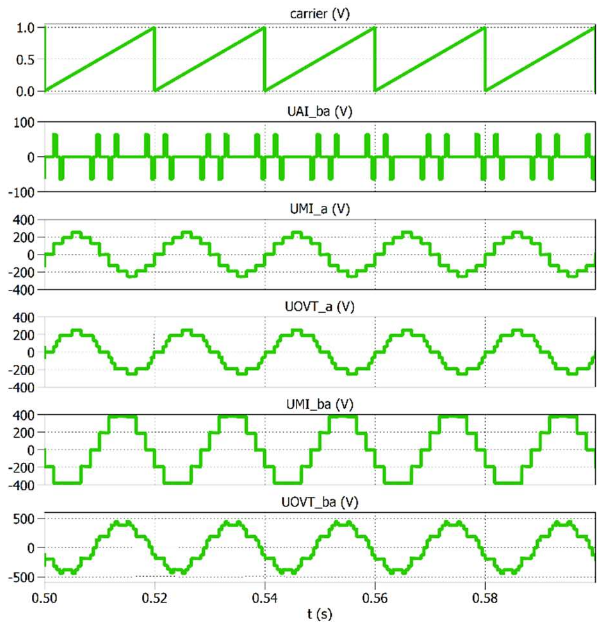

Fig.11 The waveforms of selected voltages obtained for the control strategy described by the vector map shown in Figure 7.

Figure 12, on the other hand, shows the amplitude spectra of the voltage waveforms from Figure 11. The spectra were calculated up to the 50th harmonic, in accordance with the standards. The same range was maintained in the other amplitude spectra.

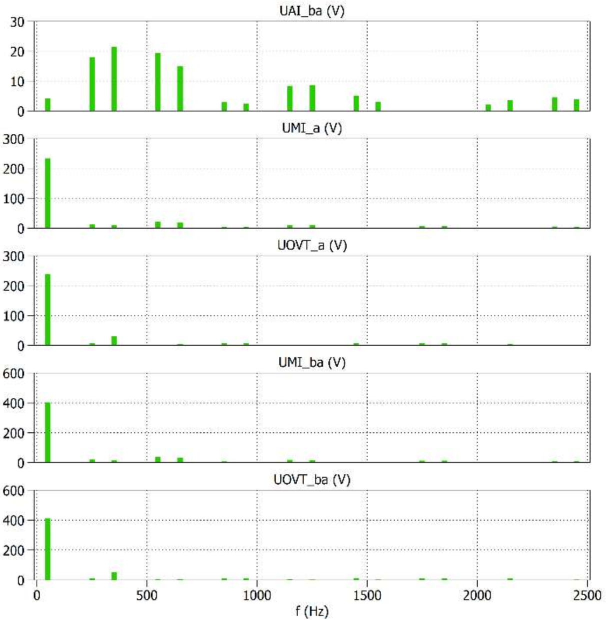

Fig.12. The amplitude spectra of the voltage waveforms from Figure 11.

Figure 13 shows the waveforms of selected voltages for the control strategy described by the vector map shown in Figure 8.

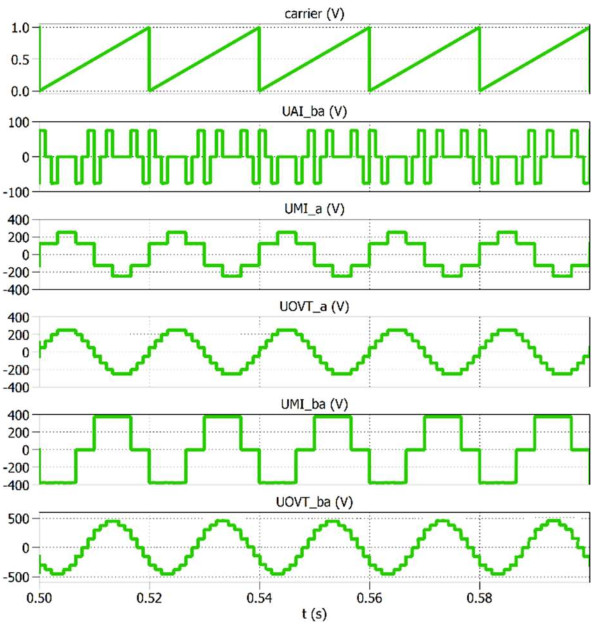

Fig.13. The waveforms of selected voltages obtained for the control strategy described by the vector map shown in Figure 8.

As before, Figure 14 shows the amplitude spectra of the voltage waveforms from Figure 13.

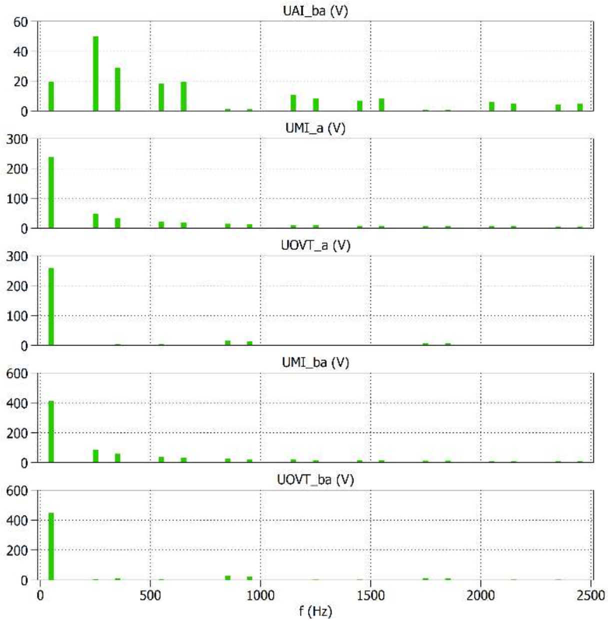

Fig.14. The amplitude spectra of the voltage waveforms from Figure 13.

In Figures 11 and 13, the comparison of the phase voltage waveforms UMI_a and UOVT_a and the set of phase-to-phase voltages UMI_ba and UOVT_ba appears particularly interesting. Table 1 presents a summary of parameters such as RMS and THD for the significant voltages resulting from the connection of the complex inverter.

Table I. - Summary of RMS and THD values for selected voltages obtained using both control strategies

Parameters	Vectors 1 (Figure 7)		Vectors 2 (Figure 8)	
	RMS	THD	RMS	THD
UMI_a	167.3	18.4	177.0	30.0
UOVT_a	169.9	13.3	184.0	9.3
UMI_ba	289.7	17.9	306.7	29.0
UOVT_ba	294.3	13.8	318.7	9.4

The simplification of the control strategy for the complex voltage inverter shows that it was a positive step towards increasing the efficiency of voltage conversion, as evidenced by the increase in the RMS value and the reduced THD content in the phase and interphase voltages generated at the output of the complex inverter.

4. Conclusion

The developed control concept for a system of three-phase inverters forming an inverter based on orthogonal vectors proves to be useful in many respects. Unlike the original concept, which involved a system of two inverters of the same type, the study demonstrated that it is also applicable to inverters of different types, such as three-level and two-level inverters.
The use of a simplified control strategy has resulted in phase and interphase voltages with a higher RMS value and a lower level of higher harmonics, as represented by THD. The use of a three-phase three-level inverter as the main inverter has provided greater control capabilities –

this inverter allows for the generation of a larger number of spatial vectors. Findings from the research indicate that an even better effect, manifested through more effective utilisation of the three-level inverter's properties, can be achieved by separating the intermediate circuits and providing a lower supply voltage for the two-level inverter and a higher supply voltage in the intermediate circuit for the three-level inverter.

References

[1] B.K. Bose, Power Electronics, Smart Grid, and Renewable Energy Systems. Proc. IEEE 2017, 105, 2011–2018. https://doi.org/10.1109/JPROC.2017.2745621.

[2] A. Łebkowski, Steam and Oxyhydrogen Addition Influence on Energy Usage by Range Extender—Battery Electric Vehicles. Energies 2018, 11, 2403. https://doi.org/10.3390/en11092403.

[3] X. Hu, J. Wang, L. Li, Y. Li, A Three-Winding Coupled-Inductor DC–DC Converter Topology With High Voltage Gain and Reduced Switch Stress. IEEE Trans. Power Electron. 2018, 33, 1453–1462 https://doi.org/10.1109/TPEL.2017.2689806.

[4] K.N.D.V.S Eswar, M.A.N.Doss, P.Vishnuram, A.Selim, M.Bajaj, H.Kotb, S. Kamel, Comprehensive Study on Reduced DC Source Count: Multilevel Inverters and Its Design Topologies. Energies 2023, 16, 18. https://doi.org/10.3390/en16010018.

[5] G.G. Kumar, M.V.S. Krishna, S. Kumaravel, E. Babaei, Multi-Stage DC-DC Converter Using Active LC2D Network With Minimum Component. IEEE Trans. Circuits Syst. II: Express Briefs 2021, 68, 943–947. https://doi.org/10.1109/TCSII.2020.3021609.

[6] K.N. Raju, M.V.G. Rao, M. Raamoorthy, Hybrid moulation technique for neutral point claped inverter to eliminate neutral 500 point shift with minimum swithing loss. In Proceedings of the TENCON 2015—2015 IEEE Region 10 Conference, Macao, China, 1–4 November 2015; pp. 1–5. https://doi.org/10.1109/TENCON.2015.7373101.

[7] Z.Xu, X. Zheng, T. Lin, J.Yao, A.Ioinvici, Switched-capacitr multilevel inverter with equal distrbution of the capacitors discharging phases. J. Electr. Eng. 2020, 6, 42–52. https://doi.org/10.23919/CJEE.2020.000029. (In Chinese)

[8] A.K.Yadav, K. Gopakumar, L. Umanand, S.Bhattacharya, W. A Jarzyna, Hybrid 7-Level Inverter Using Low-Voltage Devices and Operation With Single DC-Link. IEEE Trans. Power Electron. 2019, 34, 9844–9853. https://doi.org/10.1109/TPEL.2018.2890371.

[9] L.Dorn-Gomba, J. Guo, A. Emadi, Multi-Source Inverter for Power-Split Hybrid Electric Powertrains. IEEE Trans. Veh. Technol. 2019, 68, 6481–6494. https://doi.org/10.1109/TVT.2019.2915173.

[10] M.D. Siddique, Low Switching Frequency Based on Asymmetrical Multilevel Inverter Topology With Reduced Switch Count. IEEE Access 2019, 7, pp. 86374–86383.

[11] G.H.P. GOoi, A.I. Maswood, Z. Lim, Five-Level Multiple-Pole PWM AC–AC Converters With Reduced Components Count. IEEE Trans. Ind. Electron. 2015, 62, 4739–4748. https://doi.org/10.1109/TIE.2015.2405504.

[12] R. Sarker, A. Datta, S. A Debnath, Modified PWM Technique to Reduce Harmonic Content of Multilevel NPC Topology 769 for Medium Voltage Electric Vehicle (EV) Applications. In Proceedings of the Michael Faraday IET International Summit 2020 (MFIIS 2020), Online, 3–4 October 2020, Volume 770, pp. 19–22.

[13] T.R.Por, A.A. Rathd, S.K. Patil, Performance Analysis of Cascaded H-Bridge Multilevel Inverter with Variable Frequency ISPWM Technique. In Proceedings of the 2019 Innovations in Power and Advanced Computing Technologies (i-PACT), Vellore, India, 22–23 March 2019.

[14] A. Muc, J. Iwaszkiewicz, Scalar Voltage-Frequency Control of the OVT Inverter. Prz. Elektrotechniczny 2023, 99, 217–220. https://doi.org/10.15199/48.2023.09.42.

[15] B. Jyothi, A. Pandian, P. Bhavana, Fabrication and experimental analysis of multiple-winding transformers for multiphase supply. Meas. Control. 2020, 53, 662–678. https://doi.org/10.1177/0020294019897086.

[16] T.F. Dorazio, High phase order transmission. In Proceedings of the 1990 IEEE technical conference on Southerntier, Bing-hamton, NY, USA, 25 April 1990; IEEE: New York, NY, USA.

[17] A. Singh, J.R. Marti, Srivastava, K.D. Circuit reduction techniques in multiphase modelling of power transformers. IEEE Trans. Power Deliv. 2010, 25, 1573–1579.

[18] A. Munteanu, A. Simion, D.A. Hagianu, L. Livadaru, D. Bidei, Special three-phase to multiple different polyphase systems electric transformer. In Proceedings of the 2014 International Conference and Exposition on Electrical and Power Engineering (EPE), Iasi, Romania, 16–18 October 2014; IEEE: New York, NY, USA.

[19] M. Hartman, M. Hashad, J. Iwaszkiewicz, Developing Inverter Output Voltage Waveforms with the Help of Orthogonal Space Vectors, IEE Conference Power Electronics and Variable Speed Drives PEVD'2000, London, United Kingdom, 18–19 IX 2000.

[20] M. Hashad, J. Iwaszkiewicz, A Novel Orthogonal-Vectors-Based Topology of Multilevel Inverters. IEEE Trans. Ind. Electron. 2002, 49, pp. 868–874.

[21] A. Muc, J. Iwaszkiewicz, Active Filtering of Inverter Output Waveforms Based on Orthogonal Space Vector Theory, Energies 2022, 15(21), 7861, https://doi.org/10.3390/en15217861.

[22] A. Muc, Cooperation of various levels and three-phase voltage inverters using the theory of orthogonal space vectors, Prz. Elektrotechniczny 2024, 10, 254–257. https://doi.org/10.15199/48.2024.10.53